Pulsed Nuclear Pumping and Spin Diffusion in a Single Charged Quantum Dot

Thaddeus D. Ladd,[1,2,*] David Press,[1] Kristiaan De Greve,[1] Peter L. McMahon,[1] Benedikt Friess,[1,3] Christian Schneider,[3] Martin Kamp,[3] Sven Höfling,[3] Alfred Forchel,[3] and Yoshihisa Yamamoto[1,2]

[1]*E. L. Ginzton Laboratory, Stanford University, Stanford, California 94305, USA*

[2]*National Institute of Informatics, Hitotsubashi 2-1-2, Chiyoda-ku, Tokyo 101-8403, Japan*

[3]*Technische Physik, Physikalisches Institut, Wilhelm Conrad Röntgen Research Center for Complex Material Systems, Universität Würzburg, Am Hubland, D-97074 Würzburg, Germany*

(Received 29 December 2009; published 2 September 2010)

We report the observation of a feedback process between the nuclear spins in a single charged quantum dot under coherently pulsed optical excitation and its trion transition. The optical pulse sequence intersperses resonant narrow-band pumping for spin initialization with off-resonant ultrafast pulses for coherent electron-spin rotation. A hysteretic sawtooth pattern in the free-induction decay of the single electron spin is observed; a mathematical model indicates a competition between optical nuclear pumping and nuclear spin-diffusion. This effect allows dynamic tuning of the electron Larmor frequency to a value determined by the pulse timing, potentially allowing more complex coherent control operations.

DOI: 10.1103/PhysRevLett.105.107401 PACS numbers: 78.67.Hc, 03.65.Yz, 42.50.Ex, 76.70.Hb

Optically controlled quantum dots (QDs) are in many ways similar to atomic systems, and are therefore often regarded as strong candidates for solid-state quantum information processing. However, one key feature distinguishing QDs in group III-V semiconductors from atomic systems is the presence of a large nuclear-spin ensemble [1]. Nuclear spins cause adverse effects such as inhomogeneous broadening and non-Markovian decoherence processes. However, nuclear spins may play useful roles as well. Although methods to use QD nuclear spins directly as a quantum memory remain challenging due to the difficulty of achieving high levels of nuclear polarization, nuclear spins may provide ways to dynamically tune and lock QD-electron-spin resonances.

Several examples of manipulating nuclei to improve electron-spin coherence have recently been observed. In electrically controlled double QDs, transition processes between electron singlet and triplet states allow the manipulation of interdot nuclear-spin polarizations, improving coherent control [2–4]. In single QDs under microwave control, nuclear effects dynamically tune the electron spin resonance to the applied microwave frequency [5]. Tuning effects are also observed in two-color continuous-wave (cw) laser experiments, in which the appearance of coherent electronic effects such as population trapping are modified by nonlinear feedback processes with nuclear spins [6,7]. Finally, nuclear spins have been shown to dynamically bring ensembles of inhomogeneous QDs into spin resonance with a train of ultrafast pulses [8,9].

Here, we describe a related but different manifestation of the non-Markovian dynamics occurring between a single electron in a QD and the nuclear bath with which it interacts, with new possibilities for use in controlling nuclear effects. The effect occurs when measuring the familiar ''free-induction decay'' (FID), equivalent in this context to a Ramsey interference experiment, of a single spin in a single QD under pulsed control. The Larmor frequency of the electron spin is dynamically altered by the hyperfine interaction with QD nuclei; the nuclear polarization is in turn altered by the measurement results of the FID experiment. The result is a feedback loop in which the nuclear hyperfine field stabilizes to a value determined by the timing of the pulse sequence. In what follows, we show the experimental manifestation of this feedback loop and present a mathematical model for the effect.

The experimental apparatus is similar to that in Refs. [10,11]. The sample is grown by molecular beam epitaxy (MBE) to contain roughly 2×10^9 cm^{-2} self-assembled InAs QDs, situated roughly 10 nm above a δ-doping layer of $\sim 4 \times 10^9$ cm^{-2} Si donors. About one-third of the QDs were negatively charged by the δ-doping layer, and a single charged QD was spectroscopically isolated at around 940 nm for the experiments. As shown in Fig. 1(a), the QDs were embedded at the center of a planar GaAs microcavity ($Q \sim 200$) with 24 and 5 pairs of AlAs/GaAs $\lambda/4$ layers in the bottom and top mirrors, respectively, which served to direct the QD emission towards the collection lens and decrease the optical power required for spin rotation.

As shown in Fig. 1(b), the two spin states of the QD electron, $|\downarrow\rangle$ and $|\uparrow\rangle$, are split with a Larmor frequency $\delta_e = g_e \mu_B B_{ext}/h$ of 25.3 GHz by a 4 T magnetic field in Voigt geometry (perpendicular to the optical axis.) These states each couple optically to two trion states $|\downarrow\uparrow, \Downarrow\rangle$ and $|\downarrow\uparrow, \Uparrow\rangle$, each containing two electrons in a spin singlet and an unpaired heavy hole. We coherently manipulate the electron-spin state by applying to the QD a circularly-polarized, 4-ps optical pulse that is detuned by $\sim$150 GHz below the exciton transitions. The pulse rotates the spin between $|\downarrow\rangle$ and $|\uparrow\rangle$ [10–13]. In the basis of states shown

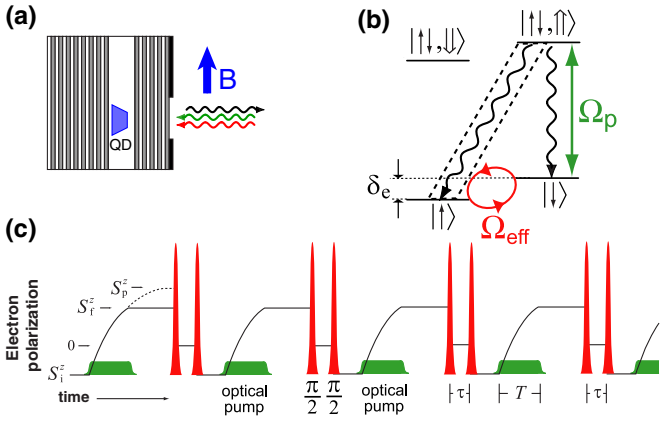

FIG. 1 (color online). (a) Sample geometry showing a single QD and a transverse magnetic field. (b) Level structure and optical interactions. Ω_p (green) labels the cw optical pump, Ω_{eff} (red) labels the pulsed coherent rotation. Wavy lines indicate spontaneous emission; the photons collected for measurement are indicated by the dashed box. (c) Periodic optical FID pulse sequence, and resulting average electron polarization. Optical pumping increases the polarization for a duration $T = 26$ ns. The saturation polarization, ($T \to \infty$, dashed line) is S_p^z; in time T only S_f^z is reached. After pumping and a short delay, a picosecond pulse (red [medium gray]) nearly instantaneously rotates the electron spin to the equator of the Bloch sphere ($\langle S^z \rangle = 0$); a time τ later a second pulse rotates the spin to achieve electron polarization S_i^z. The theoretical count rate $C(\omega, \tau)$ of Eq. (1) is found as $S_f^z - S_i^z$ in steady-state conditions.

in Fig. 1(b), the physical process may be considered a stimulated Raman transition [11,12]; for spins quantized along the optical axis, the same physical process may be considered an ac Stark shift [13]. Two timed pulses are achieved by splitting a single optical pulse with an unbalanced Mach-Zender interferometer. A retroreflector on a computer-controlled stage allows the time delay τ between the two rotation pulses to be scanned by up to 300 ps.

Before being manipulated by a sequence of rotation pulses, the spin is first initialized into the ground state $|\uparrow\rangle$ by optical pumping [Fig. 1(b)]. A 26 ns pulse from a narrow-band laser gated with an electro-optic modulator drives the $|\downarrow\rangle \leftrightarrow |\downarrow\uparrow, \Uparrow\rangle$ transition with rate Ω_p. Spontaneous decay then shelves the spin into $|\uparrow\rangle$ within a nanosecond time scale. The optical pumping step also serves to measure the spin state resulting from the previous rotation sequence: if the spin was rotated to $|\downarrow\rangle$ then a single photon will be emitted from the $|\downarrow\uparrow, \Uparrow\rangle \to |\uparrow\rangle$ transition as the spin is reinitialized. This photon is spectrally filtered by a double monochromator and detected using a single-photon counter.

After initialization into $|\uparrow\rangle$ and the first $\pi/2$ rotation, the electron spin freely precesses around the equator of the Bloch sphere at its Larmor precession frequency δ_e. The second rotation introduces a projection onto the z axis which varies sinusoidally with τ; that projection is measured during the subsequent initialization step as the entire sequence is repeated [Fig. 1(c)]. After averaging, the resulting trion count rate shows fringes as a function of τ with frequency δ_e, the expected result of an FID or Ramsey interferometer experiment. In the absence of any electron-nuclear-spin feedback mechanisms, the nuclear spins would be expected to fluctuate randomly on a time scale slow compared to the Larmor precession, leading to random Overhauser shifts of the electron's Larmor frequency due to the contact-hyperfine interaction. Time-averaged measurements would lead to the sinusoidal fringes decaying with a Gaussian shape on a time scale T_2^*. Other experiments [10] allow a separate measurement of T_2^* at about 2 ns.

However, such a Gaussian decay was not observed. Figure 2 shows the result of the FID experiment. The top three traces show the fringes seen as the delay τ is increased, and the bottom three correspond to decreasing τ. The oscillatory fringes, rather than decaying, evolve into a sawtooth pattern at high values of τ [14], and show hysteresis depending on the direction in which τ is scanned. Figure 2(b) illustrates the result of switching the scan direction.

These data result from two competing processes, which "push" and "pull" the nuclear polarization and therefore the Overhauser shift ω in contrary directions. The push process is due to trion emission, while the pull process is due to nuclear spin diffusion. In what follows, we discuss the physical origins of these processes and introduce a simple differential equation whose stable solutions model our data well.

The model relies on a separation of dynamics into three very distinct time scales. The fastest time scale is the pulse sequence and resulting electron-spin dynamics, repeated continuously with a repetition period of 143 ns, shown in Fig. 1(c). This is much faster than the nuclear dynamics we consider, which are presumed to occur on millisecond time

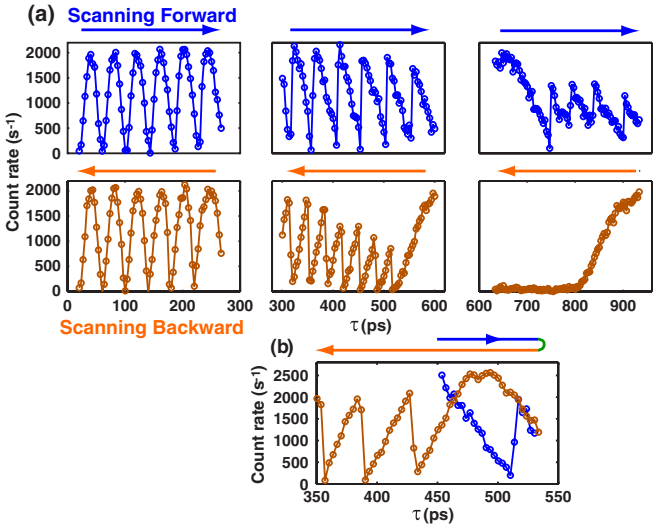

FIG. 2 (color online). (a) Experimental FID count rate as a function of two-pulse time delay τ. (b) Experimental FID fringe count rate as τ is continuously scanned longer and then shorter, showing clear hysteresis.

scales. The averaging time scale of the measurement is much longer still, on the order of several seconds, allowing the nuclei substantial time to reach quasiequilibrium.

The "push" process is due to trion recombination, as considered previously [6,9]. The dipolar interaction between a trion's unpaired hole and a nuclear spin may induce a spin flip with the nuclear Zeeman energy compensated by the broad width of the emitted photon ($\gamma/2\pi \sim 0.1$ GHz). Fermi's golden rule, in second order, allows an estimate of the rate Γ_n at which a trion hole nearly polarized along the sample growth axis (orthogonal to the magnetic field) randomly flips the nth nuclear spin during spontaneous emission, with the photonic density of states negligibly changed by the Zeeman energy of the nucleus. The result is $\Gamma_n \approx (B_n^{(\mathrm{h})}/B_0)^2\gamma$, where $B_n^{(\mathrm{h})}$ is the magnetic field at nucleus n due to the hole's dipolar field. Estimates for this field [16] are on the order of 10 G, placing Γ_n^{-1} on the order of 10 ms. In contrast, the larger contact-hyperfine field of the electron in the quantum dot is less likely to flip the nucleus during trion emission, due to the required compensation of the electron Zeeman energy at the high magnetic field (4 T) we employ.

Trion emission drives an unbiased random walk in nuclear polarization, with a *rate* proportional to the probability that a trion is created by the FID pulse sequence. The trion creation probability is plotted in the green and blue color scale of Fig. 3 as a function of pulse delay τ and Overhauser shift ω, and is described by the equation

$$C(\omega,\tau) = S_{\mathrm{p}}^{z}\frac{\{1-\exp[-\beta(\omega)T]\}\{1-\cos[(\omega_0+\omega)\tau]\}}{1-\cos[(\omega_0+\omega)\tau]\exp[-\beta(\omega)T]}. \quad (1)$$

Here, ω_0 is the electron Larmor frequency in the absence of nuclear shifts, ω is the Overhauser shift, $\beta(\omega)$ is the rate of optical pumping, T is the pumping time, and S_{p}^{z} is the saturation value of the polarized spin. The trion creation probability $C(\omega,\tau)$ oscillates sinusoidally with increasing τ due to the spin's Larmor precession. The Overhauser shift ω changes the frequency of Larmor precession. The trion creation probability drops to 0 for large values of $|\omega|$ because the trion transition shifts away from resonance with the optical pumping laser, leading to reduced pumping efficiency ($\beta(\omega) \to 0$) and trion creation.

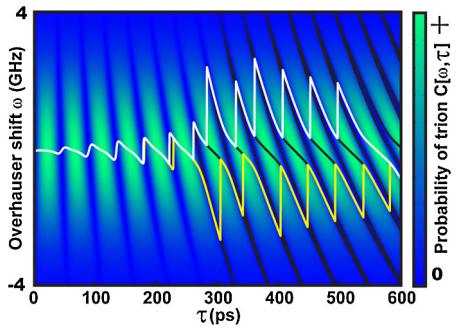

FIG. 3 (color online). Count rate $C(\omega,\tau)$ as a function of Overhauser shift ω and two-pulse delay τ. The green (light gray) areas indicate where a higher count rate is expected. Oscillations in the horizontal directions at frequency $\omega_0+\omega$ are due to Ramsey interference; the Gaussian envelope in the vertical direction is due to the reduction of optical pumping with detuning. The superimposed black lines indicate stable points where $\partial\omega/\partial t = 0$ according to Eq. (3). Superimposed on these lines are the solutions to this equation which result as τ is scanned longer (yellow [light gray] line) and shorter (white line).

The "pull" process is the presence of nuclear spin diffusion, a process known to limit nuclear polarization rates in quantum dots [17]. Modeling this process microscopically requires careful consideration of energy conservation, since the magnetic field gradient due to the hyperfine field of the electron substantially slows nuclear spin diffusion at the core of the quantum dot, but does not completely freeze it [18]. Phenomenologically, diffusion will cause nuclear polarization to "leak out" of the quantum dot at some rate κ.

As the nuclear polarization is pushed by trion emission and pulled by nuclear spin diffusion, the system quasiequilibrates to a stable value of ω that lives on the edge of the fringes shown in Fig. 3; with our separation of time scales, the nuclear polarization then "surfs" along the edge of this function as τ is changed. As τ is increased, $|\omega|$ increases causing the observable photon count to decrease due to the reduced degree of optical pumping. When $|\omega|$ is so high that pumping is ineffective ($\beta(\omega) \to 0$) and the trion-induced walk stops, spin diffusion causes the system to drift back to a new stable magnetization at a lower value of $|\omega|$, and the process continues.

This process may be formally modeled by a diffusion equation for the probability density function (PDF) of the Overhauser shift. In this model, the nuclear hyperfine shift is a random variable Ω with time-dependent PDF $f(\Omega,t)$, with average $\langle\Omega\rangle = \int d\Omega\,\Omega f(\Omega,t) = \omega(t)$. The processes we have described are captured by the equation

$$\frac{\partial f}{\partial t} = \kappa\frac{\partial}{\partial\Omega}[\Omega f] + \frac{\partial}{\partial\Omega}\left\{\left[\frac{\kappa}{2(T_2^*)^2} + \alpha C(\Omega,\tau)\right]\frac{\partial f}{\partial\Omega}\right\}. \quad (2)$$

This is a standard dissipative diffusion equation, in which the polarization is dissipated at rate κ while simultaneously fluctuating. In the absence of trion-induced feedback ($\alpha = 0$), the fluctuation rate is independent of the pulse sequence and the equilibrium solution for $f(\Omega,\tau)$ is a Gaussian distribution, which would lead the fringes of $\langle C(\Omega,\tau)\rangle$ to undergo Gaussian decay with time constant T_2^*. However, the sawtoothlike fringes we observe last for at least an order of magnitude longer than T_2^*, suggesting that the distribution $f(\Omega,t)$ is substantially narrowed. The interplay of nuclear diffusion amongst hyperfine fields and trion-induced nuclear polarization allows the system to find a stable quasiequilibrium value of Ω. To find this equilibrium value, we add the trion-induced nuclear diffusion to the fluctuation term with magnitude α estimated by $\sum_n \Gamma_n A_n^2 \approx \delta_{\mathrm{e}}^2/(1\ \mathrm{sec})$, where the sum is over nuclei and A_n is the hyperfine coupling parameter to nucleus n. We then consider the average $\omega(t)$ using Eq. (2).

To handle averaging over the nonlinear function $C(\Omega, \tau)$, we note that the experimental observation of long-lived fringes suggests $C(\Omega, \tau)$ is a sufficiently flat function of Ω in comparison to the narrowed width of $f(\Omega, t)$, in which case we may treat $C(\Omega, \tau)$ as roughly constant at $C(\omega(t), \tau)$. This assumption, which requires a narrowing of $f(\Omega, \tau)$ not fully captured by Eq. (2), also allows the system to develop hysteresis. The simple ordinary differential equation resulting from this assumption is

$$\frac{\partial \omega}{\partial t} = -\kappa\omega + \alpha \frac{\partial C(\omega, \tau)}{\partial \omega}. \quad (3)$$

Invoking our separation of time scales, we presume $\omega(t)$ evolves from its initial value (set by the last chosen value of τ) to a quasiequilibrium final value ω_f. This final value determines the expected count rate $C(\omega_f, \tau)$ at this value of τ. We solve by assuming $\omega(0) = 0$ at the first attempted value of τ, and then we scan τ up and then down as in the experiment, finding the steady-state solution of Eq. (3) at each value. For more details and justification of this model, see Ref. [19].

Figure 4 shows the modeled $C(\omega_f, \tau)$ and $\omega_f/2\pi$ as a function of τ. This particular model used $\kappa/\alpha = 10^4$ ps^{-2}, which provides the estimate $\kappa^{-1} \sim 100$ ms, a relevant time scale for dipolar-induced nuclear spin diffusion. This choice of parameters reproduces the qualitative shape of the data quite well, and quantitatively reproduces the location where sinusoidal fringes evolve into sawtoothlike fringes. Qualitative differences are dominated by the random conditions that develop when the stage is moved on its rail, forming the breaks between data sets in Fig. 2(a). Details of the shape of the waveform are related to the assumed form of the optical absorption. We used $\beta(\omega) = \beta_0 \exp(-\omega^2/2\sigma^2)$, with $\sigma/2\pi = 1.6$ GHz and $\beta_0 = 3/T$ for known pumping time $T = 26$ ns, which roughly matches the experimentally observed count rate when scanning the pump laser across the resonance. The precise absorption shape is distorted by other hysteretic nuclear pumping effects when using scanning cw lasers, as reported elsewhere [6,7].

This effect may be useful for future coherent technologies employing QDs. This pulse sequence may serve as a ''preparation step'' for a qubit to be used in a quantum information processor, as it tunes the qubit to a master oscillator [12] and narrows the random nuclear distribution, assisting more complex coherent control [2–5,8,9]; in particular, phase-controlled δ-function-like rotation pulses are promising for strong dynamical decoupling [20].

In conclusion, we have observed nonlinear nuclear feedback effects in a single charged QD resulting from the countering processes of random nuclear walks driven by trion creation, the finite width of optical absorption, Overhauser-shifted Larmor precession, and nuclear spin diffusion. Although the model we have presented is simple and replicates the data well, it requires extension to describe the processes in a QD under all possible pulse sequences. In particular, the nonlinear effects seen here are highly suppressed in spin-echo measurements [10], even though trion creation follows a similar nonlinear function to Eq. (1). Future work will involve extensions of this model to explain non-Markovian effects of nuclei under more complex pulse sequences, as well as exploiting them to extend QD-based quantum memories.

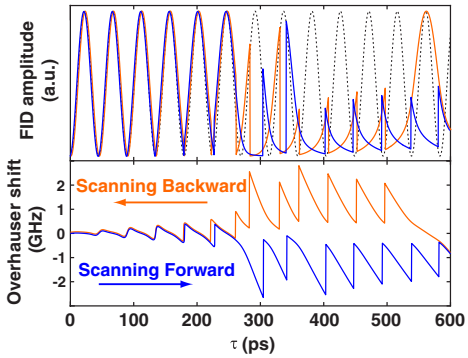

FIG. 4 (color online). (Top) The modeled count rate or FID amplitude $C(\omega_f, \tau)$. The blue (dark gray) lines and the red (light gray) lines correspond to scanning τ longer and shorter, respectively. The dotted line is the expected FID in the absence of nuclear effects. (Bottom) The Overhauser shift ω_f predicted by the model, repeated from Fig. 3.

We thank Erwin Hahn for valuable discussions. This work was supported by NICT, MEXT, NSF CCF0829694, the State of Bavaria, and Special Coordination Funds for Promoting Science and Technology.

*Present address: HRL Laboratories, LLC, 3011 Malibu Canyon Road, Malibu, CA 90265.
tdladd@gmail.com

[1] M. D. Schroer and J. R. Petta, Nature Phys. **4**, 516 (2008).
[2] F. H. L. Koppens *et al.*, Science **309**, 1346 (2005).
[3] D. J. Reilly *et al.*, Science **321**, 817 (2008).
[4] H. Bluhm *et al.*, arXiv:1003.4031.
[5] I. T. Vink *et al.*, Nature Phys. **5**, 764 (2009).
[6] X. Xu *et al.*, Nature (London) **459**, 1105 (2009).
[7] C. Latta *et al.*, Nature Phys. **5**, 758 (2009).
[8] A. Greilich *et al.*, Science **317**, 1896 (2007).
[9] S. G. Carter *et al.*, Phys. Rev. Lett. **102**, 167403 (2009).
[10] D. Press *et al.*, Nat. Photon. **4**, 367 (2010).
[11] D. Press *et al.*, Nature (London) **456**, 218 (2008).
[12] S. M. Clark *et al.*, Phys. Rev. Lett. **99**, 040501 (2007).
[13] J. Berezovsky *et al.*, Science **320**, 349 (2008).
[14] See also the top trace of Fig. 3b of Ref. [15].
[15] E. D. Kim *et al.*, Phys. Rev. Lett. **104**, 167401 (2010).
[16] J. Fischer *et al.*, Phys. Rev. B **78**, 155329 (2008).
[17] D. Gammon *et al.*, Phys. Rev. Lett. **86**, 5176 (2001).
[18] A. Z. Genack and A. G. Redfield, Phys. Rev. Lett. **31**, 1204 (1973).
[19] T. D. Ladd *et al.*, arXiv:1008.0912.
[20] K. Khodjasteh and D. A. Lidar, Phys. Rev. A **78**, 012355 (2008).